



Short communication

Non-chelating *p*-phenylidene-linked bis-imidazoline analogs of known influenza virus endonuclease inhibitors: Synthesis and anti-influenza activity

Dmitry Dar'in ^a, Vladimir Zarubaev ^b, Anastasia Galochkina ^b, Maxim Gureev ^c, Mikhail Krasavin ^{a,*}

^a Saint Petersburg State University, Saint Petersburg, 199034, Russian Federation

^b Pasteur Institute of Epidemiology and Microbiology, 14 Mira Street, Saint Petersburg, 197101, Russian Federation

^c I.M. Sechenov First Moscow State Medical University, Moscow, 119991, Russian Federation

ARTICLE INFO

Article history:

Received 25 September 2018

Received in revised form

24 October 2018

Accepted 28 October 2018

Available online 29 October 2018

Keywords:

Influenza virus

N-aryl imidazoline

Bis-imidazoline

Metal-catalyzed *N*-Arylation

In silico modeling

ABSTRACT

A novel chemotype topologically similar to known influenza virus PA endonuclease inhibitors has been designed. It was aimed to reproduce the extended topology of the known metal-chelating ligands with a *p*-phenylidene-linked bis-imidazoline scaffold. It was envisioned that aromatic groups introduced to this scaffolds via metal-catalyzed *N*-arylation (Buchwald-Hartwig or Chan-Evans-Lam) would contribute to lipophilic binding to the target and one of the imidazoline nitrogen atoms would ensure non-chelating coordination to the prosthetic divalent metal ion. The compounds displayed appreciable anti-influenza activity *in vitro* and substantial concentration window from the general cytotoxicity range. Docking analysis of low-energy poses of the most active compound (as well as their comparison to the binding of an inactive compound) revealed that these compounds reproduced similar binding components to a known PA endonuclease inhibitor and displayed similar binding pose and desired monodentate metal coordination, as was initially envisioned. These findings warrant further investigation of the mechanism of action of the newly discovered series.

© 2018 Elsevier Masson SAS. All rights reserved.

1. Introduction

Influenza is perhaps the most widespread infectious disease causing up to 500,000 deaths every year from either the disease itself or its complications [1]. Prevention of influenza by vaccination presents a formidable challenge as it can only be effective if the specific strains of the flu virus that will circulate in the forthcoming epidemic season are predicted correctly. This is particularly difficult to achieve as the variability of the virus is very high due to such factors as aerosol dissemination mechanism, existence of natural reservoirs of its circulation (birds, pigs, etc.) exacerbated by the possibility of interspecies transmission [2]. In addition, the segmented nature of viral genome allows the process of reassortment, which results in the emergence of novel gene constellations with new antigenic and pathogenic properties.

Moreover, it is the high variability within each segment itself that leads to the virus developing resistance to the existing anti-influenza drugs in the current clinical use (such as neuraminidase inhibitors, M2 channel blockers [3]). Thus, developing novel anti-influenza drugs is of a paramount importance. Thus, it is important that new and effective drug candidates, preferably with a novel mechanism of action are constantly progressed through the development pipeline.

The influenza virus polymerase acidic (PA) endonuclease is a bridged dinuclear metalloenzyme that plays a crucial role in initiating viral replication. Since it is an enzyme that is essential for the viral lifecycle, it can be considered a valid drug target for antiviral therapy development [4]. To-date, there are no anti-flu therapies with this mechanism of action with worldwide approval. However, the recent advancement of two PA endonuclease inhibitors (AL-794, S-033188, baloxavir marboxil) into the clinical studies speaks for the validity of this novel target approach [5]. The results of phase III clinical trials of baloxavir marboxil [6] confirmed it to possess superior efficacy, likely due to the novel mechanism of

* Corresponding author. Institute of Chemistry, Saint Petersburg State University, 26 Universitetsky Prospect, Peterhof, 198504, Russian Federation.

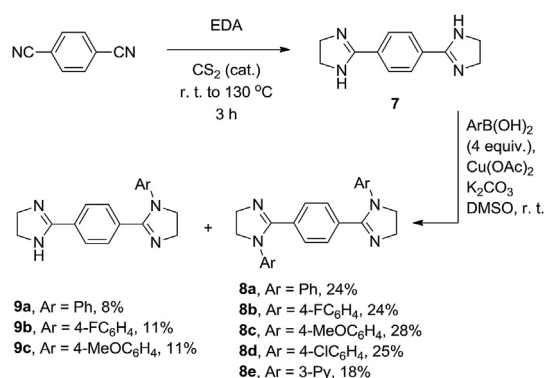
E-mail address: m.krasavin@spbu.ru (M. Krasavin).

action in contrast to other clinically available antivirals [7]. This led to the approval of baloxavir marboxil (trade name Xofluza™) in Japan in the early 2018 [8]. The majority of known PA endonuclease inhibitors incorporate a metal-chelating moiety which ensures the small molecule's affinity to the protein target containing prosthetic Mn^{2+} or Mg^{2+} ions [9]. Particularly relevant to the present study are 3-hydroxy 2-pyridone **1** [10], 5-hydroxy 4-pyrimidone **2** [11] and 3-hydroxy-4-pyridone **3** [12] compounds decorated with a *p*-phenylidene-linked *NH*-tetrazole moiety. Likewise, the clinical front-runner baloxavir marboxil (**4**) [6] also belongs to this chemical class. Being a prodrug activated *in vivo*, it possesses a metal-chelating moiety capped with a hydrolytically prone methyl carbonate moiety. At the same time, a number of non-chelating compounds (e. g., THC-19 (**5**) [13] and PA-30 (**6**) [14]) have surfaced from phenotypical screening of large compound libraries that exhibited activity against influenza virus and were shown to inhibit PA endonuclease. Although the binding mode for these compounds has not been established [4], the absence of obvious chelating motifs in their structure suggests a possibility of alternative non-chelating binding to the prosthetic divalent metals. This, in turn, inspired us to try and mimic the extended, linear arrangement of two heterocyclic motifs present in compounds **1–3** with *p*-phenylidene-linked bis-imidazoline scaffold **7** [15]. We reasoned that, while one of the imidazoline moieties could replace the *NH*-tetrazolyl motif, the other could also coordinate to the metal ion. Moreover, considering our recent developments in the area of metal-catalyzed imidazoline *N*-arylation [16,17], various aromatic and heteroaromatic substituents could be installed at the two imidazoline moieties in **7**, thus leading to additional hydrophobic and/or hydrogen-bonding interactions with the target (Fig. 1). Herein, we present the results of reducing this idea to practice, which resulted in identifying compounds endowed with pronounced anti-influenza activity and low cytotoxicity.

2. Results and discussion

2.1. Synthesis

The starting *p*-phenylidene-linked bis-imidazoline **7** was synthesized in 90% yield from terephthalonitrile and ethylene diamine via a CS_2 -catalyzed reaction, as described in the literature [18]. Bis-arylation of **7** with 4 equiv. of aryl boronic acids under the Chan-Evans-Lam conditions [17] resulted in the formation of the desired *N,N'*-bis-aryl compounds **8a–e** isolated chromatographically in moderate yield. In three cases, respective mono-arylated versions **9a–c** were also isolated (Scheme 1).

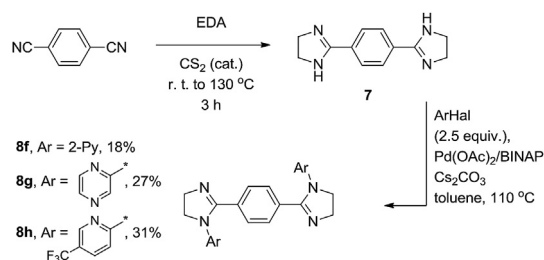


Scheme 1. Preparation of bis- (**8a–e**) and mono-arylated (**9a–c**) bis-imidazolines via the Chan-Evans-Lam arylation of **7**.

While introduction of 2-pyridyl and 2-pyrazinyl groups via the Chan-Evans-Lam arylation protocol would not be feasible due to low stability of the respective boronic acids and their tendency to de-borylation under the reaction conditions, the complementary approach [16] involving Pd-catalyzed Buchwald-Hartwig-type *N*-arylation with respective, highly reactive heteroaryl halides, was considered. Indeed, using a 2.5-fold excess of respective chloroazines, the bis-arylation reaction gave the desired compounds **8f–h** in moderate yield (Scheme 2).

2.2. Biological evaluation

The anti-influenza activity of compounds synthesized was evaluated in MDCK cells infected with A/Puerto Rico/8/34 (H1N1) strain of influenza virus. Additionally, the compounds were



Scheme 2. Preparation of bis-heteroaryl bis-imidazolines **8f–h** via the Buchwald-Hartwig arylation.

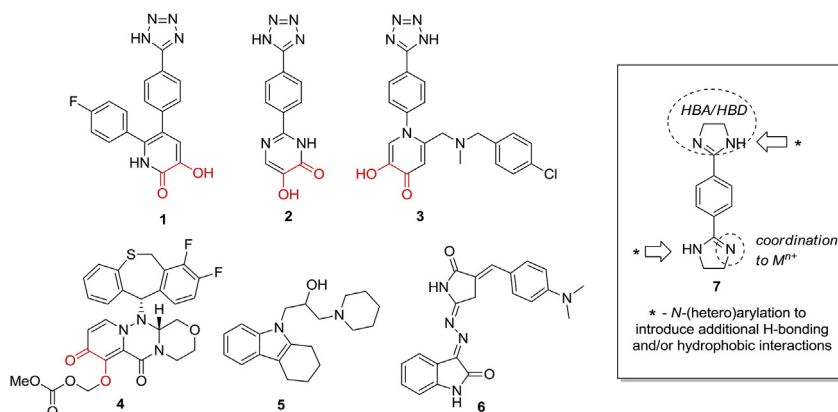


Fig. 1. Metal-chelating (**1–4**, critical portion highlighted), known non-chelating (**5–6**) influenza virus PA endonuclease inhibitors and the *p*-phenylidene-linked bis-imidazoline scaffold **7** explored in this work.

evaluated for their general cytotoxicity as the ability to cause death of uninfected MDCK cells. The resulting data expressed as IC₅₀ and CC₅₀ (μmol/L) are presented in Table 1.

Generally, both the mono- and bis-aryl series demonstrated tendency to suppress viral titer in lower concentration range than that causing reduction of mammalian MDCK cell count (see Experimental section). Preliminarily, in the bis-aryl series, the antiviral activity appears to be enhanced by introducing substitutions in the *para*-position of the phenyl ring (cf. **8a** vs. **8b-d**) and lowered by nitrogen heteroaromatics in lieu of phenyl counterparts (cf. **8e-h**). Particularly detrimental to the antiviral potency was the introduction of the second nitrogen atom (as bis-pyrazinyl analog **8g**). Also notable is the lower cytotoxicity of the mono-aryl compounds which warrants further investigation of this subclass of *p*-phenylidene-linked bis-imidazolines. Although these compounds (**9a-c**) are somewhat weaker compared to clinically used antiviral drug rimantadine, their cytotoxicity is much lower. Thus, further optimization may lower the IC₅₀ values while keeping the compounds' profile within the ample selectivity window already observed for the initial leads.

Table 1
Anti-influenza activity (IC₅₀), cytotoxicity (CC₅₀) and calculated selectivity indices (SI) of compounds **8a-h** and **9a-c** synthesized in this work.

Compound	Structure	CC ₅₀ , μM	IC ₅₀ , μM	SI
8a		>817	77	>11
8b		144	12	12
8c		361	16	23
8d		9	5	2
8e		>813	68	>12
8f		127	35	4
8g		>809	>809	–
8h		455	103	4
9a		>1031	30	>34
9b		>971	65	>15
9c		224	44	5
Rimantadine		62	11	6

2.3. Docking studies

The crystal structure of influenza virus PA endonuclease complex with compound **1** (PDB index 4M4Q) was employed in docking simulation of the binding of the most potent compounds from the mono- (**9a**) and bis-aryl series (**8b** and **8d**) in comparison with compound **8g** which is completely devoid of the desired activity. First, the key interactions of **1** with the protein were examined to reveal the importance of the *p*-fluorophenyl substituent interaction within the hydrophobic pocket lined with Ile38/Ala37/Tyr24/Met21/Ala20 residues. Additionally, electrostatic interaction of the tetrazolyl moiety with Lys34/Arg124 diad is crucial as well as interaction with the divalent metal ions present in the enzyme's active site. The latter principal component consists of π -cation interaction of the *p*-fluorophenyl group with the Mg²⁺ ion and the chelation of one of the three Mn²⁺ ions by the hydroxypyridone motif (Fig. 2).

Compound **1** was re-docked into the active site of PA endonuclease along with compounds **8b**, **8d** and **9a** (most active) as well as **8g** (inactive) studied in this work. To our delight, this led to comparably favorable energy characteristics for the active compounds (**1**, **8b**, **8d** and **9a**) and a markedly lower calculated binding energy for compound **8g**. Moreover, this is reflected in the principal components (lipophilic, van-der-Waals and Coulomb) contributing to the overall binding (Table 2).

Close examination of the orientation of active compounds **8b**, **8d** and **9a** revealed strikingly similar contribution from all three principal components: i. lipophilic pocket filling with an *N*-arylimidazole moiety (with a notable π -stacking interaction of that aryl moiety with Tyr24), ii. electrostatic interaction of the other imidazole moiety with Lys134/Lys137 diad (possibly supported by an additional π -stacking interaction with Tyr130 for **8b** and **8d**), iii. non-chelating coordination of the first (lower) *N*-aryl imidazole moiety to the active site Mg²⁺ ion via the unsubstituted nitrogen atom (Fig. 3).

In contrast to the above findings, inactive compound **8g** docked into PA active site displayed no stable binding mode and poor overlay with reference ligand **1**. The binding pose with the best GlideScore and Emodel values was characterized exclusively by a set of hydrophobic interactions with no π -stacking or metal coordination contacts (Fig. 4). This situation differs from that observed for compound **8b** whose overall binding energy was only ~0.4 kcal/mol lower compared to **8g**; compound **8b**, however, displayed rather stable docking poses and good overlay with reference ligand **1**.

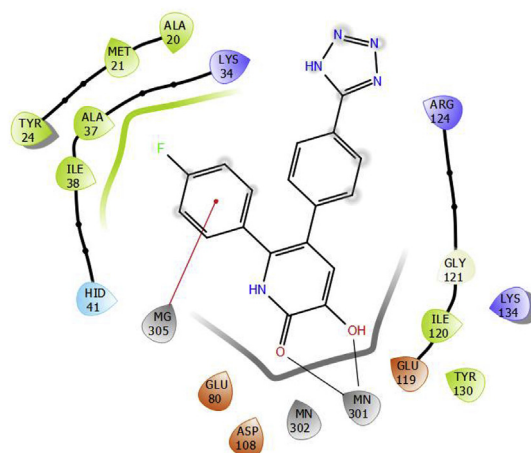


Fig. 2. Known metal-chelating PA endonuclease inhibitor **1**: two-dimensional ligand-interaction diagram (LID) showing critical interactions with the protein target.

Table 2Results of molecular docking of compounds **1**, **8b**, **8d**, **8g** and **9a** into the crystal structure of influenza virus PA endonuclease complex with **1** (PDP index 4M4Q).

Compound	GlideScore	Emodel	Lipo	VdW	Coulomb	ΔG (kcal/mol)
1	-5.517	-83.725	-0.654	-17.369	-49.449	-8.010
9a	-5.678	-80.884	-0.686	-11.644	-52.125	-8.060
8b	-5.078	-76.581	-0.555	-11.047	-49.495	-7.691
8d	-5.350	-72.198	-0.687	-16.073	-46.920	-8.079
8g	-5.917	-71.219	-0.008	-4.829	-38.469	-7.330

3. Conclusion

We described bis- and mono-arylated *p*-phenylidene-linked bis-imidazolines as a novel, non-chelating mimic of known influenza virus PA endonuclease inhibitors with similarly extended linear arrangement of heterocyclic moieties. The antiviral activity of these compounds was evaluated *in vitro* to reveal appreciable potency and significantly lower general cytotoxicity. Docking simulation of binding of the most active compounds to the target - and comparison of their binding to that of the known PA endonuclease inhibitors - revealed similar contribution from lipophilic and electrostatic components as well as non-chelating binding to the prosthetic Mg²⁺ ion of one of the imidazoline nitrogen atoms, confirming the initial design idea (preliminarily suggesting that these compounds might exert their activity through such an inhibition mechanism). This finding further extends the utility of *N*-aryl imidazoline moiety as an emerging privileged motif in drug design [19]. Further investigation of the mechanism of action of the newly discovered series of anti-influenza compounds is required and will be reported on in due course.

4. Experimental section

4.1. Chemistry

NMR spectroscopic data were recorded with Bruker Avance 400 spectrometer (400.13 MHz for ¹H and 100.61 MHz for ¹³C) in DMSO-*d*₆ and in CDCl₃ and were referenced to residual solvent proton signals ($\delta_H = 7.26$ and 2.50 ppm, respectively) and solvent carbon signals ($\delta_C = 77.0$ and 39.5 ppm, respectively). Melting points were determined with a Stuart SMP50 instrument in open capillary tubes. Mass spectra were recorded with a Bruker Maxis HRMS-ESI-qTOF spectrometer (electrospray ionization mode). Toluene was distilled from P₂O₅ and stored over molecular sieves 4 Å.

4.1.1. Synthesis of 1,4-bis(4,5-dihydro-1H-imidazol-2-yl)benzene (**7**)

To a suspension of terephthalonitrile (2.56 g, 0.02 mol) in ethylene diamine (10 mL) 5 drops of carbon disulfide were added and the mixture was stirred at room temperature for 10 min. Then the mixture was stirred at 130 °C for 3 h. Upon cooling water (50 mL) was added, the precipitate was filtered off and stirred with DMSO (60 mL) at 110 °C for 5 min. After cooling to ambient temperature crystals were filtered, washed with water and hot acetonitrile, and dried at 80 °C for overnight to afford 3.88 g (90%), colorless solid, mp 292–294 °C, lit. 312–314 °C [17]. ¹H NMR (400 MHz, DMSO-*d*₆): δ 7.85 (s, 4H), 6.91 (br.s, 2H), 3.62 (s, 8H).

4.1.2. General procedure for the preparation of compounds **8a-e** and **9a-c** (GP1)

A mixture of compound **7** (0.7 mmol), ArB(OH)₂ (2.8 mmol), Cu(OAc)₂ (2.0 mmol), K₂CO₃ (3.5 mmol) and DMSO (3 mL) was stirred in an open flask at ambient temperature for 3–5 days (reaction progress was controlled by TLC). Reaction mixture was

diluted with EtOAc (80 mL) containing Et₃N (2 mL), stirred for 10 min and filtered through a pad of celite. The filtrate was washed with water (20 mL) and brine (15 mL), dried over anhydrous Na₂SO₄ and concentrated *in vacuo*. The resulting crude material was subjected to column chromatography on silica gel to afford compounds **8a-e** and **9a-c**. Compounds **8a**, **9a** and **8d** were purified by elution with EtOAc/MeOH/Et₃N system (from 94:5:1 to 90:9:1), compounds **8b**, **9b**, **8c**, **9c** and **8e** - with EtOAc/MeOH/Et₃N system (from 90:9:1 to 80:16:4).

4.1.2.1. 1,4-Bis(1-phenyl-4,5-dihydro-1H-imidazol-2-yl)benzene (**8a**). Prepared according to GP1. Yield 61 mg (24%) as colorless solid; m.p.: 221–223 °C. ¹H NMR (400 MHz, CDCl₃): δ 7.43 (s, 4H), 7.19–7.12 (m, 4H), 6.99 (t, *J* = 7.4 Hz, 2H), 6.83–6.68 (m, 4H), 4.06 (s, 8H). ¹³C NMR (101 MHz, CDCl₃): δ 162.2, 142.7, 132.5, 128.8, 128.6, 123.6, 122.6, 54.0, 53.0. HRMS *m/z* [M+H]⁺ calcd for C₂₄H₂₃N₄ 367.1917, found 367.1913.

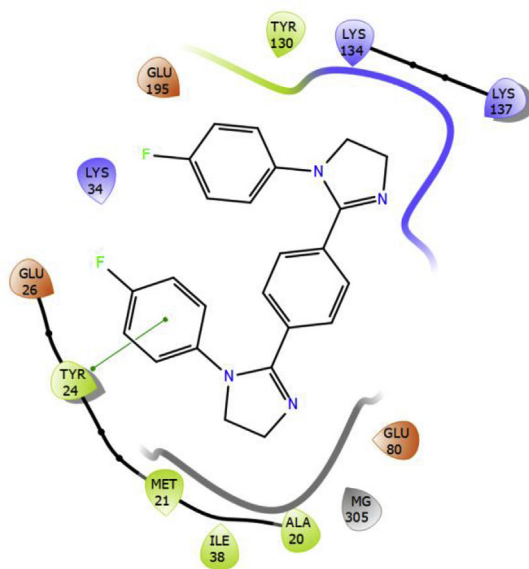
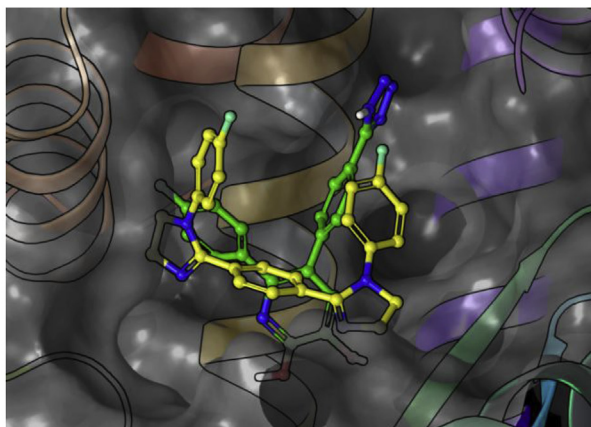
4.1.2.2. 2-(4-(4,5-Dihydro-1H-imidazol-2-yl)phenyl)-1-phenyl-4,5-dihydro-1H-imidazole (**9a**). Prepared according to GP1. Yield: 16 mg (8%) as colorless solid; m.p.: 182–184 °C. ¹H NMR (400 MHz, DMSO-*d*₆): δ 7.83 (d, *J* = 8.3 Hz, 2H), 7.51 (d, *J* = 8.3 Hz, 2H), 7.19 (t, *J* = 7.9 Hz, 2H), 7.00 (t, *J* = 7.4 Hz, 1H), 6.81 (d, *J* = 7.6 Hz, 2H), 4.14–3.86 (m, 4H), 3.71 (s, 4H). ¹³C NMR (101 MHz, DMSO-*d*₆): δ 163.9, 161.2, 143.5, 134.7, 129.5, 129.3, 128.8, 127.9, 123.8, 123.0, 54.3, 53.4, 48.5. HRMS *m/z* [M+H]⁺ calcd for C₁₈H₁₉N₄ 291.1604, found 291.1613.

4.1.2.3. 1,4-Bis(1-(4-fluorophenyl)-4,5-dihydro-1H-imidazol-2-yl)benzene (**8b**). Prepared according to GP1. Yield 68 mg (24%), colorless solid, mp 213–215 °C. ¹H NMR (400 MHz, CDCl₃): δ 7.40 (s, 4H), 6.86 (t, *J* = 8.6 Hz, 4H), 6.76 (dd, *J* = 9.0, 4.7 Hz, 4H), 4.11–4.03 (m, 4H), 4.03–3.94 (m, 4H). ¹³C NMR (101 MHz, CDCl₃): δ 162.4, 159.4 (d, *J* = 244.4 Hz), 139.1 (d, *J* = 2.9 Hz), 132.3, 128.6, 124.9 (d, *J* = 8.2 Hz), 115.7 (d, *J* = 22.6 Hz), 54.6, 53.1. HRMS *m/z* [M+H]⁺ calcd for C₂₄H₂₁F₂N₄ 403.1729, found 403.1742.

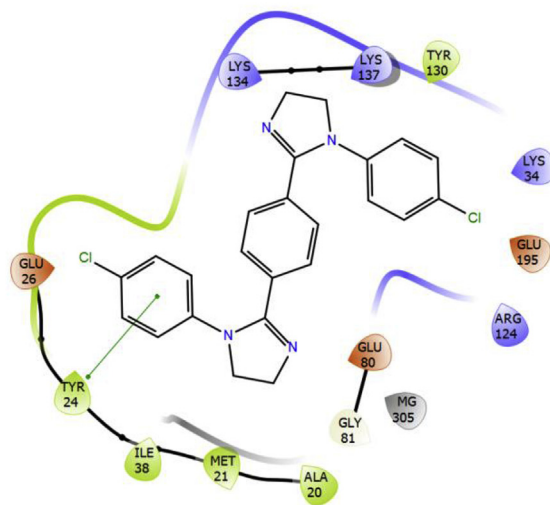
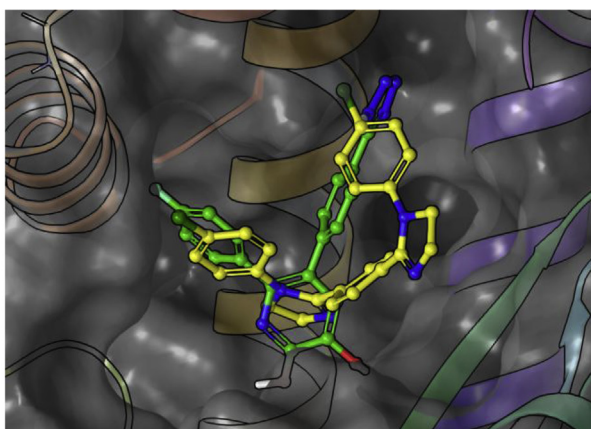
4.1.2.4. 2-(4-(4,5-Dihydro-1H-imidazol-2-yl)phenyl)-1-(4-fluorophenyl)-4,5-dihydro-1H-imidazole (**9b**). Prepared according to GP1. Yield: 23 mg (11%) as colorless solid; m.p.: 196–198 °C. ¹H NMR (400 MHz, CDCl₃): δ 7.76 (d, *J* = 8.2 Hz, 2H), 7.41 (d, *J* = 8.2 Hz, 2H), 6.75 (t, *J* = 8.6 Hz, 2H), 6.67 (dd, *J* = 8.9, 4.8 Hz, 2H), 4.02–3.92 (m, 2H), 3.91–3.83 (m, 2H), 3.73 (s, 4H). ¹³C NMR (101 MHz, CDCl₃): δ 164.3, 162.0, 159.2 (d, *J* = 244.1 Hz), 139.2 (d, *J* = 2.8 Hz), 134.2, 128.8, 128.8, 127.6, 124.9 (d, *J* = 8.2 Hz), 115.6 (d, *J* = 22.6 Hz), 54.6, 53.4, 48.3. HRMS *m/z* [M+H]⁺ calcd for C₁₈H₁₈FN₄ 309.1510, found 309.1517.

4.1.2.5. 1,4-Bis(1-(4-methoxyphenyl)-4,5-dihydro-1H-imidazol-2-yl)benzene (**8c**). Prepared according to GP1. Yield: 83 mg (28%) as colorless solid; m.p.: 211–213 °C. ¹H NMR (400 MHz, CDCl₃): δ 7.38 (s, 4H), 6.75 (d, *J* = 9.0 Hz, 4H), 6.69 (d, *J* = 9.0 Hz, 4H), 4.07–4.00 (m, 4H), 3.97–3.91 (m, 4H), 3.75 (s, 6H). ¹³C NMR (101 MHz, CDCl₃): δ 163.1, 156.5, 136.3, 132.3, 128.5, 125.2, 114.2, 55.4, 55.0, 53.1. HRMS *m/z* [M+H]⁺ calcd for C₂₆H₂₇N₄O₂ 427.2129, found 427.2136.

A



B



C

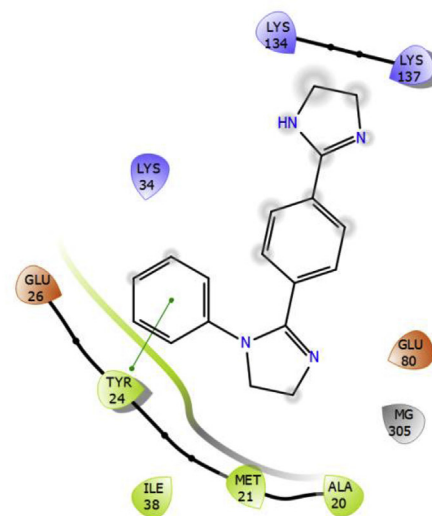
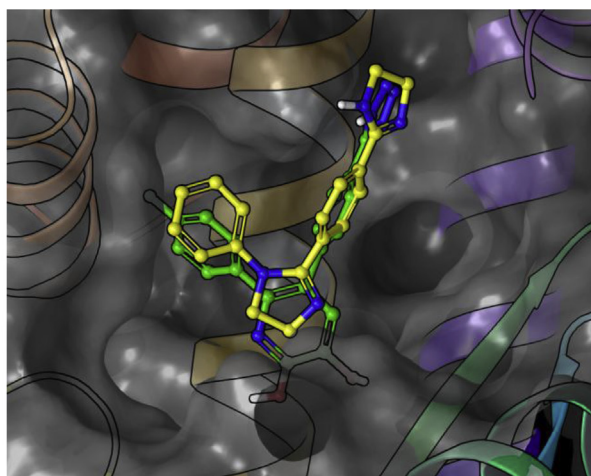


Fig. 3. Overlay of docking poses of compounds **8b** (A), **8d** (B) and **9a** (C) with compound **1** in its complex with influenza virus PA endonuclease and two-dimensional LIDs.

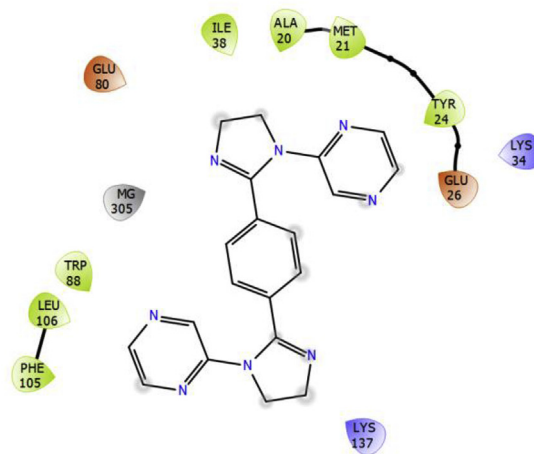
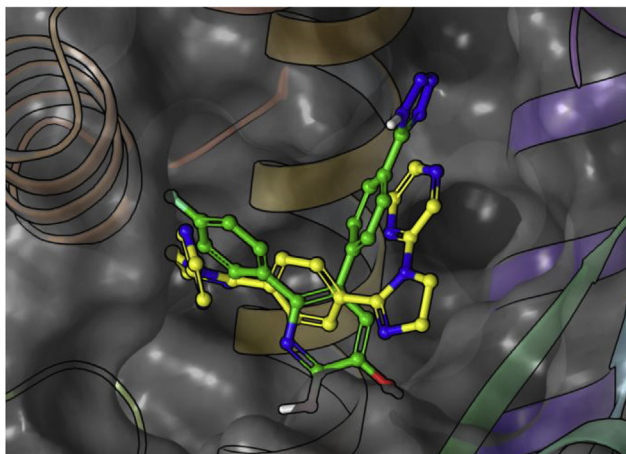


Fig. 4. Overlay of docked compound **8g** with ligand **1** in the active site of influenza virus PA endonuclease and the respective two-dimensional LID.

4.1.2.6. 2-(4-(4,5-Dihydro-1H-imidazol-2-yl)phenyl)-1-(4-methoxyphenyl)-4,5-dihydro-1H-imidazole (**9c**). Prepared according to GP1. Yield: 24 mg (11%) as colorless solid; m.p.: 191–193 °C. ¹H NMR (400 MHz, CDCl₃): δ 7.70 (d, *J* = 8.4 Hz, 2H), 7.50 (d, *J* = 8.4 Hz, 2H), 6.80 (d, *J* = 9.0 Hz, 2H), 6.72 (d, *J* = 9.0 Hz, 2H), 4.11–4.02 (m, 2H), 4.02–3.92 (m, 2H), 3.77 (s, 4H), 3.75 (s, 3H). ¹³C NMR (101 MHz, CDCl₃): δ 164.3, 163.0, 156.6, 136.4, 133.4, 131.2, 128.8, 126.8, 125.3, 114.3, 55.4, 55.1, 53.3, 50.1. HRMS *m/z* [M+H]⁺ calcd for C₁₉H₂₁N₄O 321.1710, found 321.1711.

4.1.2.7. 1,4-Bis(1-(4-chlorophenyl)-4,5-dihydro-1H-imidazol-2-yl)benzene (**8d**). Prepared according to GP1. Yield: 97 mg (32%) as colorless solid; m.p.: 222–224 °C. ¹H NMR (400 MHz, CDCl₃): δ 7.40 (s, 4H), 7.14 (d, *J* = 8.6 Hz, 4H), 6.71 (d, *J* = 8.7 Hz, 4H), 4.14–4.01 (m, 8H). ¹³C NMR (101 MHz, CDCl₃): δ 162.2, 140.5, 131.9, 129.6, 129.0, 124.5, 114.0, 53.8, 52.2. HRMS *m/z* [M+H]⁺ calcd for C₂₄H₂₁Cl₂N₄ 435.1138, found 435.1149.

4.1.2.8. 1,4-Bis(1-(pyridin-3-yl)-4,5-dihydro-1H-imidazol-2-yl)benzene (**8e**). Prepared according to GP1. Yield: 66 mg (25%) as colorless solid; m.p.: 225–227 °C. ¹H NMR (400 MHz, CDCl₃): δ 8.30–8.16 (m, 4H), 7.46 (s, 4H), 7.11–7.02 (m, 2H), 6.94 (d, *J* = 8.5 Hz, 2H), 4.19–4.02 (m, 8H). ¹³C NMR (101 MHz, CDCl₃): δ 161.3, 144.6, 143.7, 139.3, 132.4, 129.1, 128.8, 123.2, 53.5, 53.5. HRMS *m/z* [M+H]⁺ calcd for C₂₂H₂₁N₆ 369.1822, found 369.1826.

4.1.3. General procedure for the preparation of compounds **8f-h** (GP2)

A solution of catalyst (prepared by short-time stirring at 110 °C of mixture of Pd(OAc)₂ (23 mg, 0.1 mmol) and BINAP (125 mg, 0.2 mmol) in dry toluene (5 mL)) was poured into a screw-capped vessel with a suspension of compound **7** (214 mg, 1.0 mmol), corresponding chloroazine (2.5 mmol), Cs₂CO₃ (652 mg, 2.0 mmol) in the mixture of dry toluene (5 mL) and dry DMF (5 mL), filled with argon. The reaction mixture was stirred at 110 °C for 20 h. After cooling to ambient temperature mixture was diluted with EtOAc (40 mL), filtered through a pad of celite and evaporated to dryness. The resulting crude material was recrystallized from EtOAc.

4.1.3.1. 1,4-Bis(1-(pyridin-2-yl)-4,5-dihydro-1H-imidazol-2-yl)benzene (**8f**). Prepared according to GP2. Yield: 66 mg (18%) as colorless solid; m.p.: 220–222 °C (EtOAc). ¹H NMR (400 MHz, DMSO-*d*₆): δ 8.14 (ddd, *J* = 4.9, 1.9, 0.7 Hz, 2H), 7.55 (ddd, *J* = 8.3, 7.3, 2.0 Hz, 2H),

7.40 (s, 4H), 6.89 (ddd, *J* = 7.3, 4.9, 0.7 Hz, 2H), 6.57–6.42 (m, 2H), 4.14–4.09 (m, 4H), 3.96–3.91 (m, 4H). ¹³C NMR (101 MHz, DMSO-*d*₆): δ 160.0, 154.5, 148.1, 137.7, 133.9, 128.3, 117.7, 114.0, 53.3, 51.6. HRMS *m/z* [M+H]⁺ calcd for C₂₂H₂₁N₆ 369.1822, found 369.1811.

4.1.3.2. 1,4-Bis(1-(pyrazin-2-yl)-4,5-dihydro-1H-imidazol-2-yl)benzene (**8g**). Prepared according to GP2. Yield: 70 mg (27%) as colorless solid; m.p.: 229–231 °C (EtOAc). ¹H NMR (400 MHz, DMSO-*d*₆): δ 8.15 (dd, *J* = 2.5, 1.5 Hz, 2H), 8.09 (d, *J* = 2.6 Hz, 2H), 7.91 (d, *J* = 1.5 Hz, 2H), 7.47 (s, 4H), 4.22–4.11 (m, 4H), 4.04–3.99 (m, 4H). ¹³C NMR (101 MHz, DMSO-*d*₆): δ 159.2, 150.9, 142.1, 137.3, 136.1, 133.9, 128.4, 53.8, 50.9. HRMS *m/z* [M+H]⁺ calcd for C₂₀H₁₉N₈ 371.1727, found 371.1737.

4.1.3.3. 1,4-Bis(1-(5-(trifluoromethyl)pyridin-2-yl)-4,5-dihydro-1H-imidazol-2-yl)benzene (**8h**). Prepared according to GP2. Yield: 156 mg (31%) as colorless solid; m.p.: 212–214 °C (EtOAc). ¹H NMR (400 MHz, DMSO-*d*₆): δ 8.50 (d, *J* = 2.4 Hz, 2H), 7.91 (dd, *J* = 8.8, 2.6 Hz, 2H), 7.48 (s, 4H), 6.63 (d, *J* = 8.8 Hz, 2H), 4.22–4.18 (m, 4H), 4.02–3.97 (m, 4H). ¹³C NMR (101 MHz, DMSO-*d*₆): δ 159.0, 156.5, 145.4, 134.8, 133.7, 128.5, 124.6 (q, *J* = 271.0 Hz), 118.0 (q, *J* = 32.9 Hz), 113.0, 53.5, 51.2. HRMS *m/z* [M+H]⁺ calcd for C₂₄H₁₉F₆N₆ 505.1570, found 505.1588.

4.2. Biology

4.2.1. Evaluation of the anti-influenza virus activity

100 μL of the compounds dissolved in MEM with 1 μg/mL trypsin was added into wells with MDCK cells and the plates were incubated for 1 h at 36 °C at 5% CO₂. Cells were infected with 100 μL of influenza virus A/Puerto Rico/8/34 (H1N1) (m.o.i. 0.01) for 1 h. Cells were washed twice with MEM and the fresh medium containing the compounds at the same concentrations was added. The plates were kept for 24 h at 36 °C at 5% CO₂. The culture medium was used for the preparation of the series of 10-fold dilutions, fresh cells were infected with the dilutions, and the plates were incubated for 48 h at 36 °C at 5% CO₂. After 48 h 100 μL of culture fluid was transferred into the wells of round-bottom plates. 100 μL per well of 1% suspension of chicken erythrocytes in saline was added and the results were checked after 40 min incubation at room temperature. The infectious titer of the virus was considered as a reciprocal to the maximum virus dilution that caused complete erythrocytes agglutination. The decrease in the

infectious titer of the virus indicated the antiviral activity of compounds. The data obtained were used for the calculation of the 50% effective concentration of the compound, or the substance concentration that caused the two-fold decrease in the virus titer (IC_{50}), and then the selectivity index was calculated, $SI = CC_{50}/IC_{50}$. Each concentration of the compounds was tested in triplicate. The IC_{50} values for each compound were calculated by GraphPad Prism software using four-parameter logistic curve model.

4.2.2. Cytotoxicity assay

MDCK cells were seeded into 96-well plates and incubated for 24 h at 36 °C at 5% CO_2 until confluent monolayer is formed. Three-fold dilutions (300 - 4 μ M) were prepared on Eagle's minimal essential medium (MEM) from the compounds under investigation, added to the cells and incubated for 24 h at 36 °C at 5% CO_2 . The cell monolayer was washed twice with saline (0.9% NaCl) and 100 μ L of MTT solution [3-(4,5-dimethylthiazole-2)-2,5-diphenyltetrazolium bromide], 0.5 μ g/mL in MEM, were added into each well. The plates were incubated for 1 h at 36 °C, then the medium was removed and formazan pellets were dissolved in dimethyl sulfoxide (0.1 mL per well). The optical density in the wells was measured on a spectrophotometer Thermo Multiskan FC at the wavelength of 540 nm. The results obtained were used for calculating the concentration of the compound resulting in death of 50% cells in the culture (CC_{50}) using GraphPad Prism software employing the four-parameter logistic curve model.

4.3. In silico modeling

The structure of influenza H1N1 virus PA endonuclease (PDP index 4M4Q) was prepared using Schrödinger Protein Preparation Wizard to eliminate possible errors in the structure of protein-ligand complex [20]. All ligands were prepared with use of Schrödinger LigPrep module [21]. Three-dimensional structure of all compounds was generated in OPLS3e force field [22]. The receptor grid was prepared using Schrödinger Glide grid generator. The grid dimensions were similar to those of ligand (12.38 Å, in XYZ axes) with an 8 Å buffer zone. The total grid side size was 20 Å, centered on the ligand midpoint. Softening potential (VdW scaling factor) applied was 0.8 with a partial charge cutoff of 0.25. During the grid generation, metal coordination constraints were imposed. The initial docking was conducted in standard precision mode with standard conditions (VdW scaling factor, RMS deviation). The number of output poses per ligand was set at 20. For each ligand, the QM charges were computed using semi-empirical method (Mulliken charges). The best binding poses were selected based on RMSD from reference ligand [23]. The best docking solutions included in ligand-protein complex with endonuclease (4M4Q) were analyzed with MM/GBSA method [24]. All images of bound ligands were generated using Schrödinger Maestro 11.6 and Ligand Interaction Diagram Generator.

Acknowledgement

This research was supported by the Russian Foundation for Basic Research (project grant 14-50-00069). NMR and mass spectrometry studies were performed at the Research Centre for Magnetic Resonance and the Centre for Chemical Analysis and Materials Research of Saint Petersburg State University Research Park.

Appendix A. Supplementary data

Supplementary data to this article can be found online at <https://doi.org/10.1016/j.ejmech.2018.10.063>.

References

- [1] C. Cianci, S.W. Gerritz, C. Deminie, M. Krystal, Influenza nucleoprotein: promising target for antiviral chemotherapy, *Antiviral Chem. Chemother.* 23 (2013) 77–91.
- [2] M. Tonelli, E. Cichero, Fight against H1N1 influenza a virus: recent insights towards the development of druggable compounds, *Curr. Med. Chem.* 23 (2016) 1802–1817.
- [3] A.E. Fiore, A. Fry, D. Shay, L. Gubareva, J.S. Bresee, T.M. Uyeki, Antiviral agents for the treatment and chemoprophylaxis of influenza, *MMWR Recomm. Rep. (Morb. Mortal. Wkly. Rep.)* 60 (2011) 1–24.
- [4] H. Ju, J. Zhang, B. Huang, D. Kang, B. Huang, X. Liu, P. Zhan, Inhibitors of influenza virus polymerase acidic (PA) endonuclease: contemporary developments and perspectives, *J. Med. Chem.* 60 (2017) 3533–3551.
- [5] X. Wu, X. Wu, Q. Sun, C. Zhang, S. Yang, L. Li, Z. Jia, Progress of small molecular inhibitors in the development of anti-influenza virus agents, *Theranostics* 7 (2017) 826–845.
- [6] S. Portsmouth, K. Kawaguchi, M. Arai, K. Tsuchiya, T. Uehara, Cap-dependent endonuclease inhibitor S-033188 for the treatment of influenza: results from a phase 3, randomized, double-blind, placebo- and active-controlled study in otherwise healthy adolescents and adults with seasonal influenza, *Open Forum Infect. Dis.* 4 (Suppl. 1) (2017) S734.
- [7] A. Dias, D. Bouvier, T. Crépin, A.A. McCarthy, D.J. Hart, F. Baudin, S. Susack, R.W.H. Ruigrok, The cap-snatching endonuclease of influenza virus polymerase resides in the PA subunit, *Nature* 458 (2009) 914–918.
- [8] Y.A. Heo, Baloxavir: first global approval, *Drugs* 78 (2018) 693–697.
- [9] M. Carcelli, D. Rogolino, A. Gatti, L. De Luca, M. Sechi, G. Kumar, S.W. White, A. Stevaert, L. Naesens, N-acylhydrazones inhibitors of influenza virus PA endonuclease with versatile metal binding modes, *Sci. Rep.* 6 (2016) 31500.
- [10] J.D. Baumann, D. Patel, S.F. Baker, R.S.K. Vijayan, A. Xiang, A.K. Parhi, L. Martinez-Sobrido, E.J. Lavoie, K. Das, E. Arnold, Crystallographic fragment screening and structure-based optimization yields a new class of influenza endonuclease inhibitors, *ACS Chem. Biol.* 8 (2013) 2501–2508.
- [11] H.Y. Sagong, J.D. Bauman, D. Patel, K. Das, E. Arnold, E.J. LaVoie, Phenyl substituted 4-hydroxypyridazin-3(2H)-ones and 5-hydroxypyrimidin-4(3H)-ones: inhibitors of influenza a endonuclease, *J. Med. Chem.* 57 (2014) 8086–8098.
- [12] C.V. Credille, Y. Chen, S.M. Cohen, Fragment-based identification of influenza endonuclease inhibitors, *J. Med. Chem.* 59 (2016) 6444–6454.
- [13] K. Yamada, H. Koyama, K. Hagiwara, A. Ueda, Y. Sasaki, S.N. Kanesashi, R. Ueno, H.K. Nakamura, K. Kuwata, K. Shimizu, M. Suzuki, Y. Aida, Identification of a novel compound with antiviral activity against influenza A virus depending on PA subunit of viral RNA polymerase, *Microb. Infect.* 14 (2012) 740–747.
- [14] S. Yuan, H. Chu, K. Singh, H. Zhao, K. Zhang, R.Y. Kao, B. Chow, J. Zhou, B.J. Zheng, A novel small-molecule inhibitor of influenza A virus acts by suppressing PA endonuclease activity of the viral polymerase, *Sci. Rep.* 6 (2016) 22880.
- [15] V. Mirkhani, M. Moghadam, S. Tangestaninejad, H. Kargar, Rapid and efficient synthesis of 2-imidazolines and bis-imidazolines under ultrasonic irradiation, *Tetrahedron Lett.* 47 (2006) 2129–2132.
- [16] M. Krasavin, Novel diversely substituted 1-heteroaryl-2-imidazolines for fragment-based drug discovery, *Tetrahedron Lett.* 53 (2012) 2876–2880.
- [17] D. Dar'in, M. Krasavin, The Chan-Evans-Lam N-Arylation Of 2-Imidazolines, *J. Org. Chem.* 81 (2016) 12514–12519.
- [18] M. Nasr-Esfahani, M. Montazerzohori, S. Mehrizi, Efficient and one-pot catalytic synthesis of 2-imidazolines and bis-imidazolines with *p*-toluenesulfonic acid under solvent free conditions, *J. Heterocycl. Chem.* 48 (2011) 249–254.
- [19] M. Krasavin, *N*-(Hetero)aryl 2-imidazolines: an emerging privileged motif for contemporary drug design, *Chem. Heterocycl. Comp.* 53 (2017) 240–255.
- [20] G.M. Sastry, M. Adzhigirey, R. Annabhimoju, W. Sherman, Protein and ligand preparation: parameters, protocols, and influence on virtual screening enrichments, *J. Comput. Aided Mol. Des.* 27 (2013) 221–234.
- [21] M.L. Verdonk, V. Berdini, M.J. Hartshorn, W.T. Mooij, C.W. Murray, R.D. Taylor, P. Watson, Virtual screening using protein-ligand docking: avoiding artificial enrichment, *J. Chem. Inf. Comput. Sci.* 44 (2004) 793–806.
- [22] E. Harder, W. Damm, J. Maple, C. Wu, M. Reboul, J.Y. Xiang, L. Wang, D. Lupyan, M.K. Dahlgren, J.L. Knight, J.W. Kaus, D.S. Cerutti, G. Krilov, W.L. Jorgensen, R. Abel, R.A. Friesner, OPLS3: a force field providing broad coverage of drug-like small molecules and proteins, *J. Chem. Theor. Comput.* 12 (2016) 281–296.
- [23] A.E. Cho, D. Rinaldo, Extension of QM/MM docking and its applications to metalloproteins, *J. Comput. Chem.* 30 (2016) 2609–2616.
- [24] A. Suenaga, N. Okimoto, Y. Hirano, K. Fukui, An efficient computational method for calculating ligand binding affinities, *PLoS One* 7 (2012), e42846.